

# Measurement of excitation functions of proton induced reactions

## on $^{nat}\text{Mo}$ , $^{nat}\text{W}$ , and $^{nat}\text{Zn}$ up to 40 MeV

G. N. Kim <sup>al</sup>, M. U. Khandaker <sup>a</sup>, K. Kim<sup>a</sup>, K. S. Kim <sup>a</sup>, M.S. Uddin <sup>ab</sup>, M.W. Lee<sup>a</sup>, Y.S. Lee <sup>a</sup>

<sup>a</sup> *Department of Physics, Kyungpook National University, Daegu 702-701, Korea.*

<sup>b</sup> *Institute of Nuclear Science and Technology, Atomic Energy Research Establishment, Savar, GPO Box No.3787, Dhaka-1000, Bangladesh.*

### Abstract

Excitation functions for the production of various radioisotopes from proton bombardment on  $^{nat}\text{Mo}$ ,  $^{nat}\text{W}$ , and  $^{nat}\text{Zn}$  were measured using the stacked-foil activation technique for proton energies up to 40 MeV. A new data set has been given for the formation of the investigated radioisotopes. The present results were compared with the earlier reported experimental data and theoretical data taken from the ALICE-IPPE code, and found good agreement with some well measured literature values in the overlapping energy region. The thick target integral yields were also deduced from the measured cross sections. The deduced yield values compared with the directly measured thick target yield values, and found acceptable agreement. The measured cross sections of the investigated radioactive products have much importance in the field of a nuclear medicine, a thin layer activation analysis, and a trace element analysis.

### 1. Introduction

Radioisotopes with a variety of half-lives (few seconds ~ few years) are widely used in medical, agricultural, and industrial research and applications. The charged particle accelerators, especially the medium energy cyclotrons are used to produce these radioisotopes. In principle, charged particle activation experiments are carried out leading to the production of high specific activity radioisotopes, reduction of impurities, and effective use of start-up materials.

Natural molybdenum (Mo), tungsten (W), and zinc (Zn) can be used as the ideal target materials for the production of medically important radioisotopes  $^{99}\text{Mo}/^{99m}\text{Tc}$ ,  $^{186}\text{Re}$ , and  $^{67}\text{Ga}$ , respectively. The radionuclide  $^{99m}\text{Tc}$  from  $^{99}\text{Mo}/^{99m}\text{Tc}$  generator is used extensively in radio-diagnostics due to its moderate half life, suitable  $\gamma$ -energy, absence of  $\beta^-$  activity, and its ability to form various complexes which have specific affinity to different organs of the human system. About 80% of the diagnostic nuclear medicine procedures are performed

---

<sup>1</sup> Corresponding author: Tel.: +82-53-950-5320, Fax :+82-53-955-5356, e-mail: gnkim@knu.ac.kr.

using  $^{99m}\text{Tc}$  labeled compounds [1]. The parent radionuclide  $^{99}\text{Mo}$  can be produced in principle in various ways. Currently, the dominant route is neutron fission of natural or isotopically enriched  $^{235}\text{U}$  (so-called “fission-moly”), while the activation of natural or isotopically enriched Mo is the second important route. Recent survey has shown that  $^{186}\text{Re}$  is an ideal candidate for radioimmunotherapy [2-4] of its moderate  $\beta^-$  particle energies at 1.07 and 0.933 MeV, low- abundance (9%)  $\gamma$  emission at 137 keV, which allows for in vivo tracking of the radiolabeled biomolecules and estimation of dosimetry calculation. The suitable 3.7-day half-life allows sufficient time for the synthesis and shipment of potential radiopharmaceuticals. On the other hand, the metallic radionuclide  $^{67}\text{Ga}$  forms strong metal complex and is of considerable interest in diagnostic nuclear medicine, particularly for tumor localization.

Several investigations [5-15] were carried out for the determination of reaction cross-sections leading to radionuclide production; but large discrepancies are found among these data set. On a practical level, it is very difficult to estimate the causes of discrepancies among the data sets. These inconsistencies severely limit the reliability of data evaluations. However, nowadays only a few groups are engaged with the systematic investigations by using modern experimental techniques and methods. Until now, no recommended data are available for the mentioned radionuclides in the literature. We therefore, investigated the production cross sections of the medically important radionuclides  $^{99m}\text{Tc}$ ,  $^{186}\text{Re}$ , and  $^{67}\text{Ga}$  from the proton bombardment of natural Mo, W, and Zn, respectively, by using the MC-50 cyclotron at the Korea Institute of Radiological and Medical Sciences (KIRAMS). The integral yields were also obtained from the respective threshold for the produced radionuclides by using the measured excitation functions as a function of proton energy.

## 2. Experimental Procedure

### 2.1. Targets and Irradiations

Excitation functions for the proton-induced reactions on natural target elements (Mo, W, Zn) were measured by using the well established stacked foil activation technique. High purity metallic form of molybdenum (>99.99%), tungsten (99.99%), zinc (99.98%), copper (>99.98%) and aluminum (99.999%) foils with natural isotopic compositions were assembled in stacks. Al and Cu foils were used as monitor as well as energy degraders. An Al foil (200  $\mu\text{m}$  thickness) was placed as the front foil of each stack (where the beam energy is well defined) to accurately measure the beam flux.

Special care was taken in preparation of uniform targets with known thickness, determination of proton energy and intensity along the stacks, and also in determination of the activities of the samples. The thickness of Mo, Zn, Cu, and Al foils was 100  $\mu\text{m}$  but that of W was 200  $\mu\text{m}$ . Several and individual stacks of natural Mo, Zn, and W with monitors were

assembled and separately irradiated by 42 MeV collimated proton beam of 10 mm diameter from the external beam line of the MC-50 cyclotron at KIRAMS. The beam intensity was kept constant during irradiation. It was necessary to ensure that equal areas of monitor and target foils intercepted the beam. The irradiation geometry was kept in a position so that the foils get the maximum beam line. To avoid errors in the determination of the beam intensity and energy, excitation functions of the monitor reactions were measured simultaneously with the reactions induced on natural molybdenum.

## 2.2. Measurement of Radioactivity

After the irradiations and appropriate waiting time the samples were taken off, and the induced gamma activities emitted from the activation foils were measured by using a gamma spectrometer. The gamma spectrometer was an n-type coaxial ORTEC (PopTop, Gmx20) high-purity germanium (HPGe) detector. The HPGe detector was coupled with a 4096 multi-channel analyzer (MCA) with the associated electronics to determine the photo peak area of the gamma-ray spectrum. The spectrum analysis was done using the program Gamma Vision 5.0 (EG&G Ortec). The energy resolution of the detector was 1.90 keV full width at half maximum (FWHM) at the 1332.5-keV peak of  $^{60}\text{Co}$ . The photopeak efficiency curve of the gamma spectrometer was calibrated with a set of standard sources:  $^{109}\text{Cd}$  (88.03 keV),  $^{57}\text{Co}$  (122.06 keV and 136.47 keV),  $^{137}\text{Cs}$  (661.65 keV),  $^{54}\text{Mn}$  (834.85 keV),  $^{22}\text{Na}$  (511.01 keV and 1274.54 keV),  $^{60}\text{Co}$  (1173.24 keV and 1332.50 keV), and  $^{133}\text{Ba}$  (80.99 keV, 276.39 keV, 302.85 keV, 356.02 keV, and 383.82 keV). The measured detection efficiencies were fitted by using the following function:

$$\ln \varepsilon = \sum_{n=0}^7 a_n \ln E^n, \quad (1)$$

where  $\varepsilon$  is the detection efficiency,  $a_n$  represents the fitting parameters, and E is the energy of the photo peak. The detection efficiencies as a function of the photon energy were measured at 10 cm and 20 cm distances from the end-cap of the detector. Since most of the sources  $^{133}\text{Ba}$ ,  $^{60}\text{Co}$ ,  $^{57}\text{Co}$  and  $^{22}\text{Na}$  emit more than one gamma ray; there is a certain probability of coincidence losses of cascade gamma rays when the sources are put closer to the detector [16]. For this reason, all samples were counted at distances of 10 cm and 20 cm from the end-cap of the detector to avoid coincidence losses, to assure low dead time (<10%) and point like geometry.

The proton beam intensity was determined from the measured activities induced in aluminum and copper monitor foils at the front position of each stack using the reactions  $^{27}\text{Al}(p,x)^{24}\text{Na}$  and  $^{\text{nat}}\text{Cu}(p,x)^{62}\text{Zn}$ , respectively. The use of the multiple monitor foils decreases the probability of introducing unknown systematic errors in activity determination. It was

considered that the loss of proton flux was very small and very hard to deduce practically. The beam intensity was considered constant to deduce cross sections for each foil in the stack. The loss of proton beam energy for each foil in the stack was calculated by using the computer program SRIM-2003 [17].

The excitation functions for the  $^{99m}\text{Tc}$ ,  $^{186}\text{Re}$ , and  $^{67}\text{Ga}$  radionuclides were determined in the proton energy range 2.5~42 MeV by using the well-known activation formula [18]. Most of the decay data regarding induced radioactivity, such as the half-life ( $T_{1/2}$ ), the  $\gamma$ -ray energy ( $E_\gamma$ ) and the  $\gamma$ -ray emission probability ( $I_\gamma$ ), were taken from the Table of Radioactive Isotopes [19], and are furnished in Table 1. The threshold energies given in Table 1 were taken from the Los Alamos National Laboratory, T-2 Nuclear Information Service on the internet [20]. The standard cross section data for the monitors were taken from internet service [21].

Table 1 Decay data of the produced radioisotopes.

Nuclei	Half-life $T_{1/2}$	Decay mode (%)	$\gamma$ -ray energy, (keV)	$\gamma$ -ray intensity( $I_\gamma$ ) (%)	Contributing reactions	Q-value (MeV)
$^{99}\text{Mo}$	2.74 d	$\beta^-$	140.511	4.52	$^{100}\text{Mo}(p, pn)$	-8.29
			181.0	6.07	$^{100}\text{Mo}(p, d)$	-6.07
			739.5	12.13	$^{100}\text{Mo}(p, 2p)$ $^{99}\text{Nb} \rightarrow ^{99}\text{Mo}$	-11.14
$^{99m}\text{Tc}$	6.02 h	$IT+\beta^-$	140.5	89.06	$^{100}\text{Mo}(p, 2n)$	-7.71
					$^{100}\text{Mo}(p, pn)$ $^{99}\text{Mo} \rightarrow ^{99m}\text{Tc}$	-8.29
					$^{100}\text{Mo}(p, d)$ $^{99}\text{Mo} \rightarrow ^{99m}\text{Tc}$	-6.06
$^{186}\text{Re}$	3.72 d		137.16	9.42	$^{186}\text{W}(p, n)$	-1.36
$^{67}\text{Ga}$	3.26 d	EC	184.6	21.2	$^{67}\text{Zn}(p, n)$	-1.81
			300.2	16.8	$^{68}\text{Zn}(p, 2n)$	-12.16
					$^{70}\text{Zn}(p, 4n)$	-28.08
$^{62}\text{Zn}$	9.186 h	EC	548.35	15.2	$^{63}\text{Cu}(p, 2n)$	-13.27
			596.7	25.7	$^{65}\text{Cu}(p, 4n)$	-31.09
$^{65}\text{Zn}$	244.26 d	EC	1115.5	50.6	$^{65}\text{Cu}(p, n)$	-2.13
$^{24}\text{Na}$	14.96 h	$\beta^-$	1368.598	100	$^{27}\text{Al}(p, p+^3\text{He})$	-23.71
					$^{27}\text{Al}(p, 2p+d)$	-29.20
					$^{27}\text{Al}(p, 3p+n)$	-31.43
$^{22}\text{Na}$	2.60 y	EC	1274.53	99.94	$^{27}\text{Al}(p, d+\alpha)$	-20.29
					$^{27}\text{Al}(p, \alpha+pn)$	-22.51

The theoretical data were taken from the MENDL-2P database [22] calculated by using the ALICE-IPPE code. It is an 'a-priori' model calculation. The calculation of cross-section using this code was based on the evaporation Weisskopf-Ewing model and geometry dependent hybrid exciton model [23]. Pre-equilibrium cluster emission calculation is included in this code. The lack of angular momentum and parity treatments in the Weisskopf-Ewing

formalism used in these codes makes independent treatment of isomeric states impossible, only total production cross-sections were calculated.

In the present experiment, all the errors were considered as independent. Consequently, they were quadratically added according to the laws of error propagation to obtain total errors. However, some of the sources of errors are common to all data, while others individually affect each reaction. The estimated major sources of errors considered in deduction of cross-sections are as follows; statistical error (1-13%), error of the monitor cross sections (2~ 4%), error due to the beam flux (2~ 4%), error due to the beam energy (0.5-1 %), error due to the detector efficiency (0.5~3%), and error due to the gamma ray intensity (1~2%). The overall uncertainty of the cross-section measurements is around 12%. The total uncertainties of the measured cross-sections were calculated by combining the statistical uncertainties ( $\delta_{sts}$ ) and other uncertainties ( $\delta_{oth}$ ).

### 3. Results and Discussion

The stable isotopes of molybdenum, tungsten, and zinc transmute to the corresponding  $^{99m}\text{Tc}$ ,  $^{186}\text{Re}$ , and  $^{67}\text{Ga}$  radioisotopes through the (p, xn) process, respectively. In some cases, two or more  $\gamma$ -rays were used for the measurement of each reaction cross-section, and the average value is presented. The detailed situations of the individually studied nuclides are discussed in the following section. The excitation functions of the investigated radioactive products are presented together with the available literature data and ALICE-IPPE prediction [22]. The numerical data with errors are collected in [Table 1](#). The integral yields were deduced using the measured cross-sections taking into account that the total energy is absorbed in the targets.

#### 3.1. Production of $^{99m}\text{Tc}$

The production cross-section of medically important radionuclide  $^{99m}\text{Tc}$  is determined through the analysis of 140.51 keV gamma-ray peak. Basically, this radionuclide can be produced in two processes. One is direct process through the reaction  $^{100}\text{Mo}(p, 2n)^{99m}\text{Tc}$  and the other is indirect process via  $^{100}\text{Mo}(p, pn)^{99}\text{Mo} \rightarrow ^{99m}\text{Tc}$  reaction. Also theoretically, the reaction  $^{98}\text{Mo}(p, \gamma)^{99m}\text{Tc}$  has little contribution in the production cross section of  $^{99m}\text{Tc}$ . The present result of  $^{99m}\text{Tc}$  radionuclide formation is shown in Fig. 1. We didn't find agreement with the data reported by Lagunas-Solar [7]. In the lower energy region (<28 MeV) the trend of peak formation agrees with our data, but at higher energy it seems to us that he didn't separate the contribution of  $^{99}\text{Mo}$  and  $^{90}\text{Nb}$  radionuclides from 140.5 keV gamma-ray peak. At higher energy (>28 MeV), the radionuclides  $^{99}\text{Mo}$  and  $^{90}\text{Nb}$  has more contribution than  $^{99m}\text{Tc}$  at 140.5 keV gamma line. This may be the possible reason to get the complete disagreement compare to our data in the higher energy region. The data reported by Scholten

et al. [6] shows general good agreement with our data. In their experiment, they worked with the 97.4% and 99.5% enriched  $^{100}\text{Mo}$  and  $^{98}\text{Mo}$  sample, respectively, but we performed the present experiment using natural molybdenum target and normalized the data for  $^{100}\text{Mo}$ . The data reported by Levkovskji [24] showed agreement at 20-30 MeV proton energy but at lower energy (<20 MeV), a clear disagreement exists not only with our data but also with the other literature values. The present measurement showed very good agreement with the recent literature data reported by Takacs et al. [25] up to 27 MeV but after then an acceptable disagreement is found, and we could not determine any possible reason. Our previous data [26] were consistent with the present data except one point around 17 MeV. Although the  $^{99\text{m}}\text{Tc}$  radionuclide has great practical importance, the production cross-sections measured by several groups showed considerable discrepancies. An accurate experimental data base is thus crucial to consider the feasibility of this reaction for a possible production of  $^{99\text{m}}\text{Tc}$  at a cyclotron.

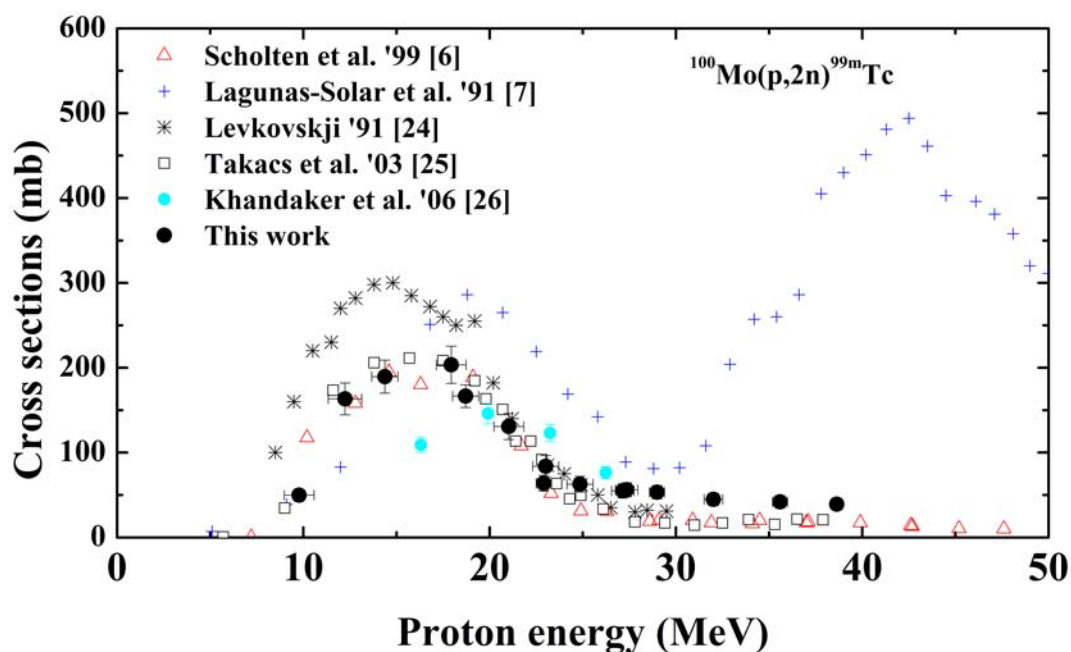


Fig. 1. Excitation function of the  $^{nat}\text{Mo}(p, xn)^{99\text{m}}\text{Tc}$  reaction.

### 3.2. Production of $^{186}\text{Re}$

The most suitable reaction path for the production of  $^{186}\text{Re}$  from the proton bombardment on natural tungsten is  $^{186}\text{W}(p, n)^{186}\text{Re}$  ( $Q = -1.069$  MeV). The measured excitation function for the production of neutron rich therapeutic radionuclide  $^{186}\text{Re}$  has shown in Fig. 2 together with the available experimental values and theoretical data taken from ALICE-IPPE code [22]. We found a very good agreement with the data reported by Lapi et al. [11], Tarkanyi et al. [27], Szelecsenyi et al. [28], and Shigeta et al. [10] in the

investigated energy region. The data reported by Zhang et al. [12] and ALICE-IPPE prediction [22] showed lower values in the peak formation region at 6-13 MeV.

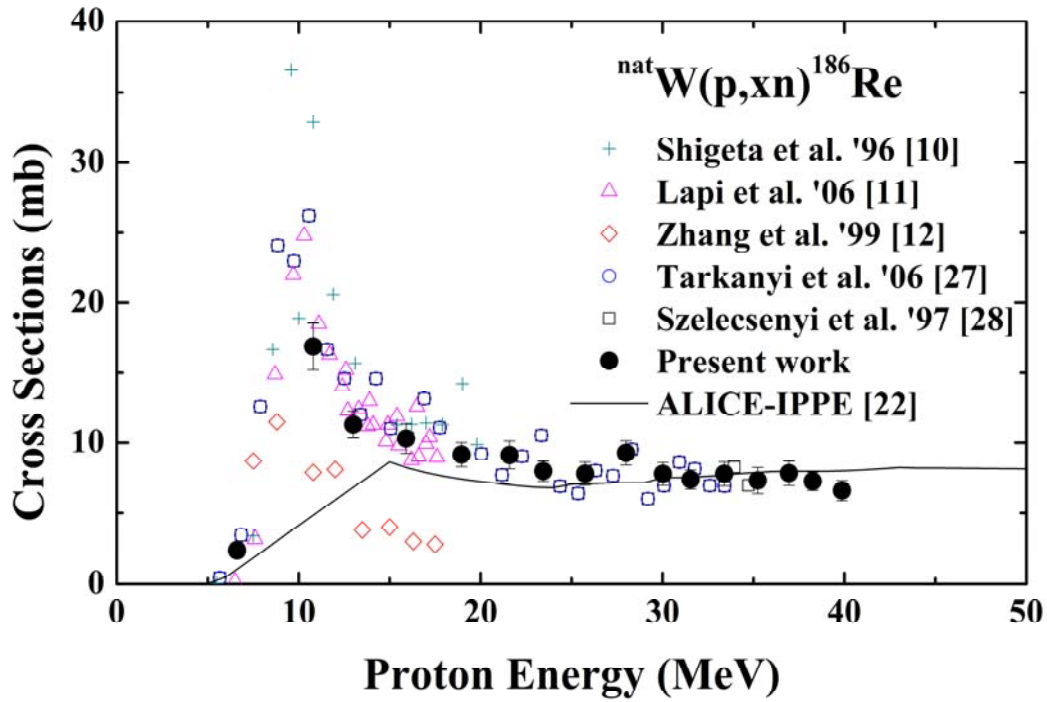


Fig. 2 Excitation function of the  ${}^{\text{nat}}\text{W}(p, xn){}^{186}\text{Re}$  reaction

### 3.3. Production of ${}^{67}\text{Ga}$

The radionuclide  ${}^{67}\text{Ga}$  is formed via the (p,2n) reactions on  ${}^{68}\text{Zn}$ . Targetry and chemical processing problems have been well studied. For the production on a small scale the (p,n) reaction on  ${}^{67}\text{Zn}$  has also been utilized. The  ${}^{67}\text{Ga}$  nuclei emitted several strong gamma-rays with different energies (184, 300, 393 keV), the activities were evaluated separately by using all these gamma-lines and the average of the individual values were taken. In the case of the  ${}^{\text{nat}}\text{Zn}(p,xn){}^{67}\text{Ga}$  process three reactions,  ${}^{67}\text{Zn}(p,n){}^{67}\text{Ga}$  ( $Q=-1.8\text{MeV}$ ),  ${}^{68}\text{Zn}(p,2n){}^{67}\text{Ga}$  ( $Q=-12.15\text{MeV}$ ) and  ${}^{70}\text{Zn}(p,4n){}^{67}\text{Ga}$  ( $Q=-27.7\text{MeV}$ ) contribute to the formation of  ${}^{67}\text{Ga}$  over the investigated proton energy range. The cross section values for the  ${}^{\text{nat}}\text{Zn}(p,xn){}^{67}\text{Ga}$  process measured in this work from 4 to 40 MeV are shown in Fig. 3 compared with the results of the previous works [13-15, 29-33] and the theoretical calculation using the ALICE-IPPE code [22]. The maximum cross section for the  ${}^{\text{nat}}\text{Zn}(p,xn){}^{67}\text{Ga}$  process was found at around 20 MeV. The  ${}^{68}\text{Zn}(p,2n){}^{67}\text{Ga}$  process has a large contribution to the  ${}^{67}\text{Ga}$  nuclide formation in peak region at about 20 MeV. Due to the low isotopic abundance of  ${}^{67}\text{Zn}$  in the natural zinc target, the  ${}^{67}\text{Zn}(p,n){}^{67}\text{Ga}$  process has lower contribution than  ${}^{68}\text{Zn}(p,2n){}^{67}\text{Ga}$ . Comparing the present results with the available previous works it can be concluded that the values of

Hermanne et al. [14, 29] are systematically higher than the present ones as well as the other investigators [15, 30, 31] above 15 MeV, but their results are in excellent agreement both with this work and Kopecky [30] below 15 MeV. The present measurement for the  $^{\text{nat}}\text{Zn}(p,xn)^{67}\text{Ga}$  process agrees well with the measurements of Tarkanyi et al. [15], Kopecky [30], and Nortier et al. [31]. The theoretical calculation using the ALICE-IPPE code [22] and this work agrees well except three points in maxima.

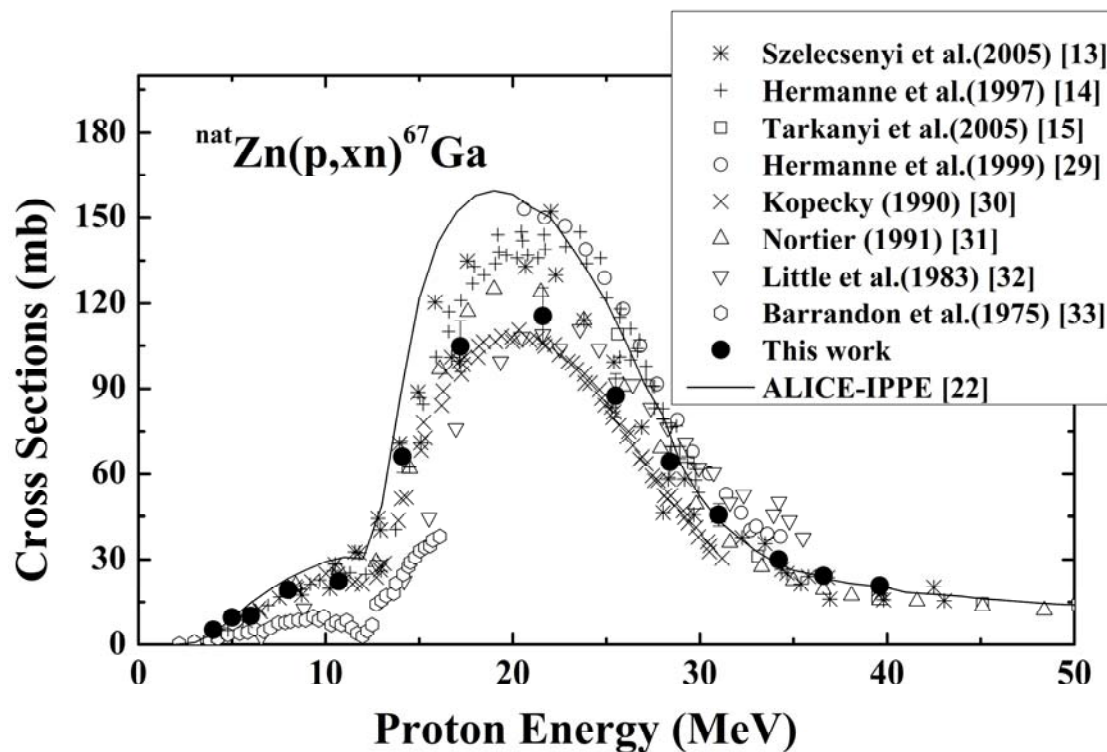


Fig. 3 Excitation function of the  $^{\text{nat}}\text{Zn}(p, xn)^{67}\text{Ga}$  reaction.

#### 4. Integral yield

The integral yield of the radionuclides from a nuclear process was deduced using the excitation function and stopping power of  $^{\text{nat}}\text{Mo}$ ,  $^{\text{nat}}\text{W}$ , and  $^{\text{nat}}\text{Zn}$  over the energy range from threshold upto 40 MeV. It is expressed as  $\text{MBq } \mu\text{A}^{-1}\text{h}^{-1}$ , i.e. for an irradiation at beam current of  $1 \mu\text{A}$  for 1 hour. The obtained results are shown in Figs. 4-5 as a function of proton energy. Dmitriev et al. [34] reported thick target yields of the  $^{67}\text{Ga}$  radionuclide measured by irradiating thick natural zinc target with 22 MeV proton beam. The used target was thick enough to cover the energy range from threshold to 22 MeV. Our results as shown in Fig. 5 are consistent with the directly measured values of Dmitriev et al. [34]. We couldn't compare the yield of  $^{99\text{m}}\text{Tc}$  and  $^{186}\text{Re}$  due to the lack of available literature values.

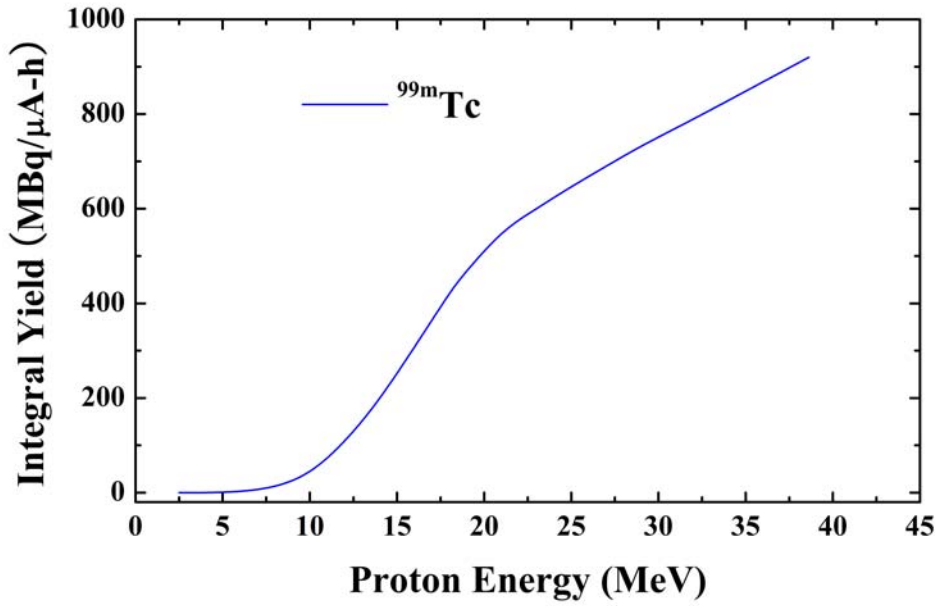


Fig. 4 Integral yield for the production of  $^{99m}\text{Tc}$  radionuclide

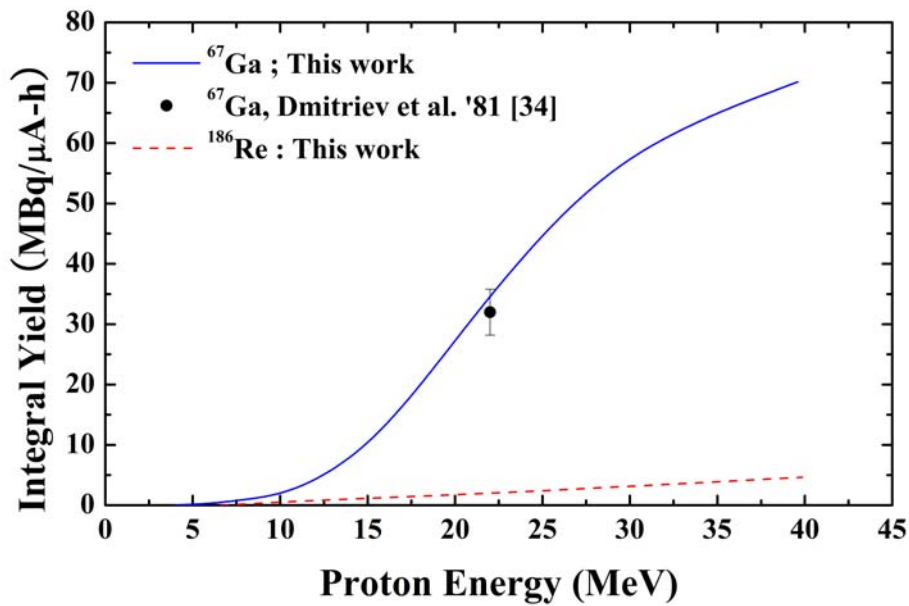


Fig. 5 Integral yields for the production of  $^{186}\text{Re}$  and  $^{67}\text{Ga}$  radionuclides

## 5. Conclusions

A new cross sections data set for the formation of  $^{99m}\text{Tc}$ ,  $^{186}\text{Re}$ , and  $^{67}\text{Ga}$  radionuclides have been reported in the energy range 2.5 - 40 MeV using the stacked-foil activation technique with an overall uncertainty of about 12%. The present experimental data were compared with the available literature values in order to select the most reliable data sets

for optimization of production routes. A considerable discrepancies still exists among the available literature data for the production of medically (SPECT) important  $^{99m}\text{Tc}$  radionuclide, which demands more and more experimental data to obtain a recommended data set, and the present data is important in this regard. Rhenium-186 ( $^{186}\text{Re}$ ) is one of the most useful radionuclide for internal radiotherapy in nuclear medicine. The measured production cross sections data of this radionuclide will help effectively to optimize the production conditions. Significant amount of  $^{67}\text{Ga}$  can be produced at low energy accelerators using natural zinc as a target, but the possibility to involve impurity of gamma emitting radionuclides is very high. The present experiment reported a reliable data set for these radionuclides in the whole investigated energy region, and these data could help in the prediction, optimization and evaluation of the radiochemical purity.

The thick target integral yields for each radionuclide were deduced using the respective measured cross-sections data. We could not compare the present values of  $^{99m}\text{Tc}$  and  $^{186}\text{Re}$  radionuclides due to the lack of available directly measured thick target yield (TTY) values in the literature. It should be mentioned that our calculated yield values can be used for the optimization of production yields of corresponding radionuclide with minimum impurity contamination. Above all, the present experimental results will play an important role in enrichment of literature data set for all of the investigated radio radionuclides.

### **Acknowledgements**

The author would like to express their sincere thanks to the staffs of the MC50 Cyclotron Laboratories for their cordial help in performing the experiment. This work was partly supported by the Korea Science and Engineering Foundation (KOSEF) through a grant provided by the Korean Ministry of Science & Technology (MOST) in 2007 (Project No. M2 07M040001110 and M2 07B020000810) and by the user program of the Proton Engineering Frontier Project (Project No. M2 02AK010014-07A1101-01419).

### **References**

- [1] W.C. Eckelman, W.A. Volkert, *Int. J. Appl. Radiat. Isot.* 33 (Special Issue) (1982) 945.
- [2] S. Kinuya, K. Yokoyama, M. Izumo, T. Sorita, T. Obata, H. Mori, K. Shiba, N. Watanabe, N. Shuke, T. Michigishi, N. Tonami, *Cancer Lett.* 219 (2005) 41.
- [3] S. Kinuya, K. Yokoyama, M. Izumo, T. Sorita, T. Obata, H. Mori, K. Shiba, N. Watanabe, N. Shuke, T. Michigishi, N. Tonami, *J. Cancer Res. Clin. Oncol.* 129 (2003) 392.

- [4] E.J. Postema, P.K. Borjesson, W.C. Buijs, J.C. Roos, H.A. Marres, O.C. Boerman, R. de Bree, M. Lang, G. Munzert, G.A.V. Dongen, W.J. Oyen, *J. Nucl. Med.* 44 (2003)1690.
- [5] S.M. Kormali, D.L. Swindle, E.A. Schweikert, *J. Radiat. Chem.* 31 (1976) 437.
- [6] B. Scholten, R.M. Lambrecht, M. Cogneau, H. Vera Ruiz, *Appl. Radiat. Isot.* 51 (1999) 69.
- [7] M.C. Lagunas-solar, P.M. Kiefer, O.F. Carvacho, C.A. Lagunas, Y.P. Cha, *Appl. Radiat. Isot.* 42 (1991) 643.
- [8] F. Roesch, S.M. Qaim, *Radiochim. Acta.* 62 (1993) 115.
- [9] N.C. Schoen, G. Orlov, R.J. McDonald, *Phys. Rev., Part C* 20 (1979) 88.
- [10] N. Shigeta, H. Matsuoka, A. Osa, M. Koizumi, M. Izumo, K. Kobayashi, K. Hashimoto, T. Sekine, R.M. Lambrecht, *J. Radioanal. Nucl. Chem.* 85 (1996) 205.
- [11] S. Lapi, W.J. Mills, J. Wilson, S. McQuarrie, J. Publicover, M. Schueller, D. Schyler, J.J. Ressler, T.J. Ruth, *App. Radiat. Isot.* 65 (2007) 345.
- [12] X. Zhang, W. Li, K. Fang, W. He, R. Sheng, D. Ying, W. Hu, *Radiochim. Acta* 86 (1999) 11.
- [13] F. Szelecsenyi, G.F. Steyn, Z. Kovacs, T.N. Van der Walt, K. Suzuki, K. Okada, K. Mukai, *Nucl. Instr. and Meth.* **B 234** (2005) 375.
- [14] A. Hermanne, Private communication, reported in Szelecsenyi et al. (1998), *Appl. Radiat. Isot.* **49** (1997)1005.
- [15] F. Tarkanyi, F. Ditroi, J. Csikai, S. Takacs, M. S. Uddin, M. Hagiwara, M. Baba, Yu. N. Shubin, A. I. Dityuk, *Appl. Radiat. Isot.* **62** (2005) 73.
- [16] A. Wyttenbach, *J. Radioanal. Nucl. Chem.* 8 (1971) 335.
- [17] J.F. Ziegler, J.P. Biersack, U. Littmark, SRIM 2003 code, Version 96.xx. The stopping and range of ions in solids. Pergamon, New York. Available at <http://www.srim.org/>
- [18] G. Gilmore, J.D. Hemingway, *Practical Gamma-Ray Spectrometry*, John Wiley & Sons, England, Chapter 1, 1995, p. 17.
- [19] E. Browne, R.B. Firestone, *Table of Radioactive Isotopes*, in: V.S. Shirley (ed.), Wiley, New York, (1986).
- [20] Reaction Q-values and thresholds, Los Alamos National Laboratory. Available from < <http://t2.lanl.gov/data/qtool.html> >
- [21] Monitor cross-section data. Available at < <http://www-nds.iaea.org/medical/> >
- [22] A.I. Dityuk, A. Yu. Konobeev, V.P. Lunev, Yu.N. Shubin, *New Advanced Version of Computer Code ALICE-IPPE, INDC(CCP)-410*, IAEA, Vienna (1998) ; *Medium Energy Activation Cross Sections data: MENDL-2P*, Available at: <<http://www-nds.iaea.org/nucmed.html>>
- [23] M. Blann, H.K. Vonach, *Phys. Rev. C*28 (1983) 1475.

- [24] V.N. Levkovskij, Middle Mass Nuclides ( $A=40-100$ ) Activation Cross-sections by Medium Energy ( $E=10-50\text{MeV}$ ) Protons and Alpha Particles (Experiment and Systematics). Inter-vesi, Moscow (1991).
- [25] S. Takacs, Z. Szucs, F. Tarkanyi, A. Hermanne, M. Sonck, J. Radioanal. Nucl. Chem. **257** (2003) 195.
- [26] M.U. Khandaker, A.K.M.M.H. Meaze, K. Kim, D. Son, G.N. Kim, Y.S. Lee, J. Korean Phys. Soc. **48** (2006) 821.
- [27] F. Tarkanyi, S. Takacs, F. Szelecsenyi, F. Ditroi, A. Hermanne, M. Sonck, Nucl. Instr. and Meth. B **252** (2006) 160.
- [28] F. Szelecsenyi, S. Takacs, F. Tarkanyi, M. Sonck, A. Hermanne, in: J.R. Heys, D.G. Mellilo, Chichester, et al. (Eds.), Proceedings of the Sixth International Symposium on Synthesis and Applications of Isotopically Labelled Compounds, Philadelphia, USA, 14–18 September, 1997, John Wiley and Sons, 1998, p. 701
- [29] A. Hermanne, F. Szelecsenyi, M. Sonck, S. Takacs, F. Tarkanyi, P. Van der Winkel, J. Radioanal. Nucl. Chem. **240** (1999) 623.
- [30] P. Kopecky, Appl. Radiat. Isot. **41** (1990) 606.
- [31] F. M. Nortier, S. J. Mills, G. F. Steyn, Appl. Radiat. Isot. **42** (1991) 353.
- [32] F. E. Little, M. C. Lagunas-Solar, Int. J. Appl. Radiat. Isot. **34** (1983) 631.
- [33] M. Yagi, K. Kondo, Int. J. Appl. Radiat. Isot. **30** (1979) 569; J. N. Barrandon, J. L. Debrun, A. Kohn, R. H. Spear, Nucl. Instr. and Meth. **127** (1975) 269.
- [34] P. P. Dmitriev, G. A. Molin, Vop. At. Nauki i Tekhn., Ser. Yadernye Konstanty **44** (1981 ) 43 (in Russian).